# A Theoretical Study on the Half-life of Bound-State Beta Decay of Long-Lived Fission Products

Konstantinos Volanis[1], Sunjoo Yoon[1], Yonghee Kim[1*], David Mascali[2], Angelo Pidatella[2] and Bharat Mishra[2]

[1]*Department of Nuclear & Quantum Engineering, Korea Advanced Institute of Science and Technology (KAIST), 291 Daehak-ro, Yuseong-gu, Daejeon 34141, Republic of Korea*
[2]*Istituto Nazionale di Fisica Nucleare, Laboratori Nazionali del Sud, Via S. Sofia 62, 95123 Catania, Italy*
[*]*Corresponding author: yongheekim@kaist.ac.kr*

***Keywords :*** bound-state beta decay, half-life, fission products,

## 1. Introduction

It is well known that $\beta^-$ decay is a weak interaction process that allows the conversion of a neutron into a proton with the creation of an electron and an antineutrino in the continuum state. However, in 1947, Daudel et al. [1] first proposed the concept of bound-state $\beta^-$ decay (BSBD), suggesting the possibility of nuclear $\beta^-$ decay accompanied by the creation of an electron directly in an unoccupied atomic orbital. This process, known as two-body decay or the time-mirrored orbital electron capture (EC) process, involves the antineutrino carrying the entire decay energy (Q value) without altering the atomic charge state.

In neutral atoms, inner orbits are fully occupied, thereby making BSBD improbable due to the Pauli exclusion principle. However, under stellar environments with high-temperature conditions and elements with high atomic numbers, atoms may become partially or fully ionized, resulting in vacancies in atomic orbits. These conditions can also lead to a depression in the ionization potential, altering the Q-value of $\beta^-$ transitions and affecting the charge state distribution of atoms. In such scenarios, BSBD may become the dominant decay branch.

The first successful experimental observation of BSBD was demonstrated at the GSI accelerator [2] in 1992, where fully stripped Dy-163 was stored in a heavy-ion storage ring and found to have a half-life of 47 days, despite Dy-163 being stable in its neutral state. Similarly, BSBD for fully ionized Re-187 was observed, which proved to be helpful in calibrating a Re-187 and Os-187 galactic chronometer [3]. In the neutral case Re-187 decays with a half-life of $4.12\ E+10$ years, whereas in the bare case, it was measured to be $32.9 \pm 2$ years. These observations suggest that the new beta decay process can be hugely accelerated compared to the conventional continuum $\beta^-$ decay of neutral atoms.

## EFFECTS ON FISSION PRODUCT DECAY [4]

As commonly known, nuclear reactors generate thousands of fission products with the majority being short-lived. However, only a few pose significant concerns regarding radiological hazards and underground disposal. Notably, isotopes like iodine and cesium are volatile, potentially leading to their release into the biosphere during severe accidents and presenting ongoing challenges for their long-term storage in repositories. Table I illustrates the primary long-lived fission products (LLFPs). While isotopes like Sr-90, Cs-137, and Sm-151 are not exceptionally long-lived, their significant production and radiotoxicity in nuclear reactors justify careful consideration. It is worth noting that total mass of all LLFPs is only about 11% of the total fission product mass and most of the LLFPs are not effectively transmutable in nuclear reactors since the transmutation cross-section is very low.

Table I: Major Long-Lived Fission Products

| Nuclide | $T_{1/2}^{neutral}$ (Year) | Production* [kg/Gwth·yr] | Radiotoxicity (Sv/g) |
|---|---|---|---|
| Se-79 | 3.2E+5 | 0.066 | 8.259 |
| Sr-90 | 28.9 | 6.07 | 1.269E+5 |
| Zr-93 | 1.6E+6 | 8.04 | 1.045 |
| Tc-99 | 2.1E+5 | 8.54 | 6.056E-1 |
| Pd-107 | 6.5E+6 | 2.34 | 1.048E-3 |
| Sn-126 | 2.3E+5 | 0.30 | 6.306 |
| I-129 | 1.6+7 | 1.96 | 2.696E-1 |
| Cs-135 | 2.3E+6 | 2.76 | 8.532E-2 |
| Cs-137 | 30.1 | 10.65 | 4.190E+4 |
| Sm-151 | 90 | 0.15 | 1.281E+2 |

*3.2% U-235 enrichment, 33 GWD/tU, 20-year cooling

Takahashi and Yokoi [5] investigated Bound-State Beta Decay (BSBD) in heavy atoms (A=59-210) within high-temperature stellar plasma, crucial for astrophysical nucleosynthesis. They provided beta decay constants for highly ionized atoms across a temperature range of $0.5 \times 10^8 K$ to $5 \times 10^8 K$. BSBD's impact on the effective half-life of LLFPs was analyzed, revealing significant acceleration of most LLFPs' beta decay, except for Sr-90 and Sn-126, shown in Table II. Sr-90 decay remained largely unaffected due to its lower atomic number and unique nuclear characteristics. The rest of the isotopes experienced ultra-acceleration, potentially reducing their effective half-life to a few years or less. This concept becomes clearer when examining Figures 1 to 5, which illustrate the ratio of the effective decay rate ($\lambda_b^{eff}$) to the neutral decay rate

($\lambda_b^{neutral}$) across varying temperatures. It's crucial to note that the atoms are not fully ionized at a temperature of $5 \times 10^8 K$. The effectiveness of the BSBD process heavily relies on the specific atomic and nuclear properties of each nuclide.

Table II: Possible Impacts of BSBD on LLFP Half-life

| Nuclide | $T_{1/2}^{BSBD}$ $(5 \times 10^8 K)$, Year | $T_{1/2}^{BSBD}$ $(5 \times 10^8 K)$/ $T_{1/2}^{neutral}$ |
|---|---|---|
| Se-79 | 0.9 | 1.45E-5 |
| Sr-90 | 29 | 1.0 |
| Zr-93 | 11,000 | 0.07 |
| Tc-99 | 0.48 | 2.3E-6 |
| Pd-107 | 9.6 | 1.5E-6 |
| Sn-126 | 53,000 | 1.9 |
| I-129 | 0.34 | 2.1E-8 |
| Cs-135 | 5.5 | 1.8E-6 |
| Cs-137 | 2.5 | 0.08 |
| Sm-151 | 0.7 | 7.9E-3 |

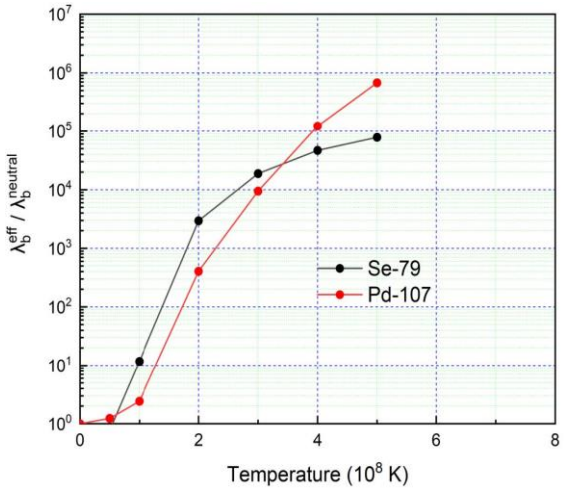


Figure 1. Decay constant ratio vs. temperature (Pd-107& Se-79).

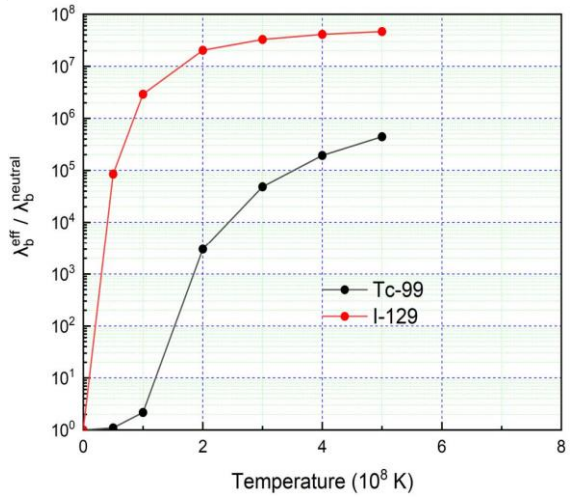


Figure 2. Decay constant ratio vs. temperature (I-129 & Tc-99).

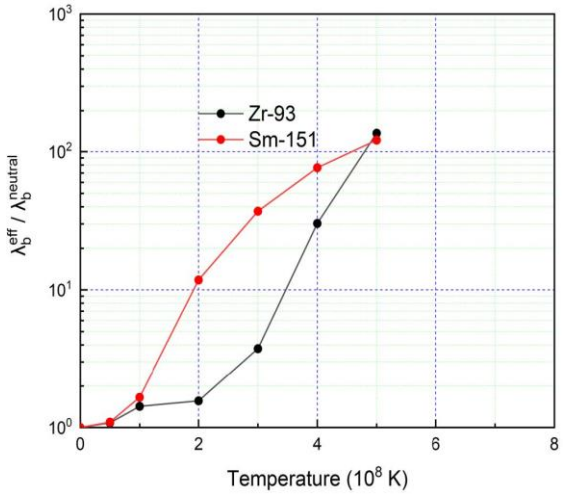


Figure 3. Decay constant ratio vs. temperature (Sm-151 & Zr-93).

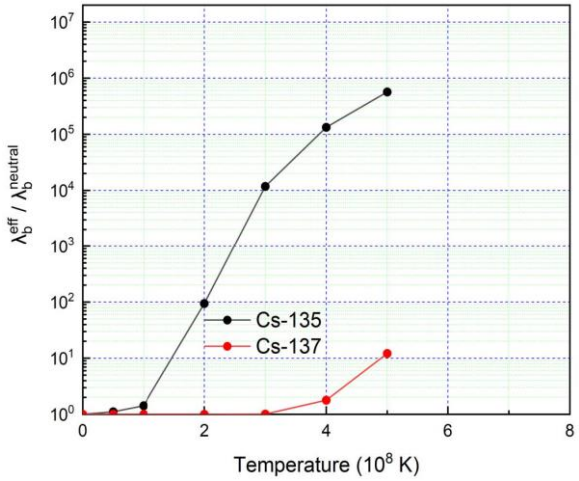


Figure 4. Decay constant ratio vs. temperature (Cs-135 & 137).

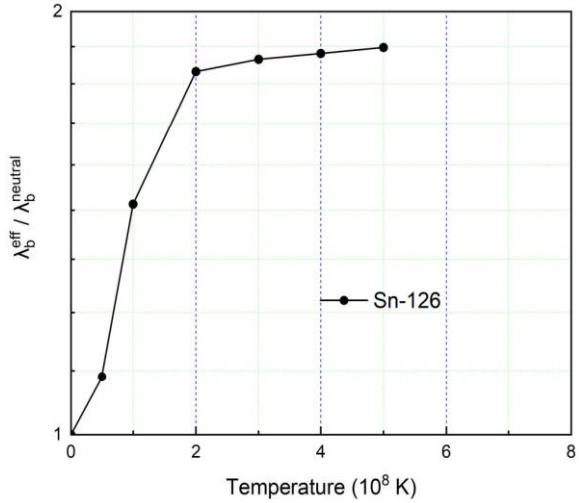


Figure 5. Decay constant ratio vs. temperature (Sn-126).

Implication of the BSBD-based ultra-accelerated decay of LLFPs will be huge in view of the nuclear fuel

cycle and waste management. To practically utilize the BSBD process, three crucial technologies are indispensable. Separation and extraction of LLFPs from the spent fuels through pyro-processing, efficient and cost-effective ionization process, and storage of heavily ionized LLFP ions, possibly in a tokomak-like device or circular arrangement of magnetic mirrors with permanent magnets, for a specified duration.

In this paper, we will be examining the scenario involving the bare atoms of these specific LLFPs.

## 2. Methods and Results [6]

In this segment, we will illustrate the Takahashi-Yokoi model utilized to compute the half-life of fully ionized LLFPs, under the assumption that that they are stored in a vacuum, absent of any plasma conditions. In our case, we do not consider the continuum state $\beta^-$ transitions since its contribution is minimal in the bare case.

The bound-state $\beta^-$decay rates $\lambda_B$ of above candidate nuclei can be calculated by:

$$\lambda_B = [ln2/(ft)]f_m^*, \quad m = a, nu, u, \tag{1}$$

where $m = a, nu, u$ stand for allowed, non-unique forbidden and unique forbidden transitions, $ft$ is the comparative half-life and $f_m^*$ the lepton phase volume, which accounts for the complete position-momentum parameter space associated with each decay channel. $ft$ values were obtained from an updated publication of atomic data and nuclear tables [7]. $f_m^*$ can be described as below,

$$f_m^* = \sum \sigma_x \left(\frac{\pi}{2}\right) [f_x or\ g_x]^2 [Q_b/m_e c^2]^2 S_{(m)x}, \tag{2}$$

where $\sigma_x$ is the vacancy of orbital $x$, $[f_x or\ g_x]^2$ denotes the square of radial wavefunction evaluated at the nuclear surface $R = 1.2 \times A^{1/3}$, $Q_b$ signifies the bound-state beta decay energy, which will be discussed further and $S_{(m)x}$ represents the shape factor of the transition.

$[f_x or\ g_x]$ can be obtained by solving the Dirac bound-state radial equations,

$$P' + \frac{kP}{r} + \left(2c + \frac{V-\varepsilon}{c}\right) Q = 0, \tag{3}$$
$$Q' - \frac{kQ}{r} - \left(\frac{V-\varepsilon}{c}\right) P = 0. \tag{4}$$

Here $E$ is the energy of electron excluding its rest energy $m_e c^2$, while the quantum number $\kappa$ is associated with the orbital angular-momentum quantum number $l$ and the total angular-momentum quantum number $j$ by,

$$\kappa = (l - j)(2j + 1) = (j + 1/2)\sigma, \tag{5}$$
$$\sigma \equiv -sgn(\kappa) = -|\kappa|/\kappa, \tag{6}$$
$$j = |\kappa| - 1/2 = l + \sigma/2, \tag{7}$$
$$l = (|\kappa| - (1 + \sigma)/2 = j - \sigma/2 \tag{8}$$

For a Coulomb potential $V = Z/r$, the above equations can be solved in terms of confluent hypergeometric functions in the form,

$$P(r) = \left(2 - \frac{\varepsilon}{c^2}\right)^{\frac{1}{2}} \xi \left(\frac{\rho}{N}\right)^{\gamma} e^{-\frac{\rho}{2N}} \times [-n_r F_1 + (N - \kappa) F_2] \tag{9}$$

$$Q(r) = -\left(\frac{\varepsilon}{c^2}\right)^{\frac{1}{2}} \xi \left(\frac{\rho}{N}\right)^{\gamma} e^{-\frac{\rho}{2N}} [n_r F_1 + (N - \kappa) F_2]. \tag{10}$$

These radial wave functions are related to the functions of $f_x$ or $g_x$ by,

$$f_x = \left(\frac{\tilde{\lambda}_c}{a_0}\right)^{3/2} \frac{P(R)}{R}, \quad g_x = \left(\frac{\tilde{\lambda}_c}{a_0}\right)^{3/2} \frac{Q(R)}{R}. \tag{11}$$

$\tilde{\lambda}_c$ and $a_0$ are the reduced Compton wavelength and Bohr radius, respectively. In Figure 6, we observe the larger component $[f_x or\ g_x]^2$ (or electron density) of various electron orbitals plotted against atomic units for Br-79, the daughter nucleus of Se-79. It's evident that the influence of $np_{1/2}$ wave functions is minimal, whereas the K shell's $(1s_{1/2})$ contribution is predominant. This trend holds true for the other daughter nuclei listed in Table I of the radionuclides.

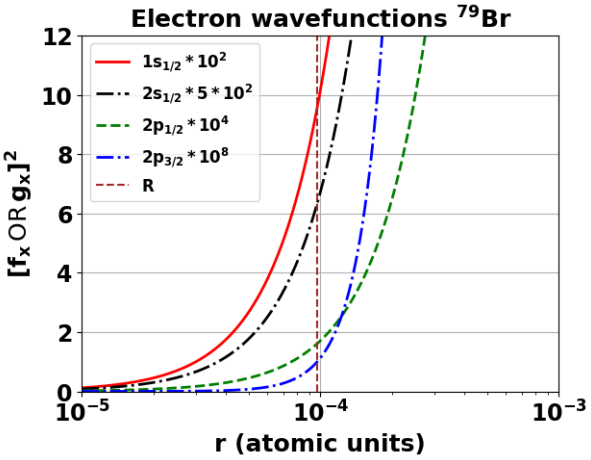


Figure 6. The squared larger components of the electron radial wave functions for different electron orbitals for Br-79.

Moreover, $S_{(m)x}$, which incorporates the conservation of spin-parity and the selection rules governing the decay process, is given by,

$$S_{(m)x} = \begin{cases} 1 & for\ m = a, nu\ and\ x = ns_{1/2}, np_{1/2} \\ q^2 & for\ m = u\ and\ x = ns_{1/2}, np_{1/2} \\ 9/R^2 & for\ m = u\ and\ x = np_{3/2}, nd_{3/2}, \end{cases} \tag{12}$$

otherwise, it is zero. If the electron is created in a higher atomic shell with large angular momentum, the impact of the transition is negligible.

The bound-state beta decay energy ($Q_b$) can be described with a more a condensed form of the general Q-value equation, as,

$$Q_b = Q_{n,m} + \Delta_{\varepsilon}{}^{ij}, \tag{13}$$

where $Q_{n,m}$ represents the neutral Q-value, $m$ stands for both ground state and excited states transitions and $\Delta_{\varepsilon^{ij}}$ is the difference in binding plus level excitation energies. To obtain these two terms, we utilized the FLYCHK software which provides information on the plasma spectroscopy developed by NIST [8]. By specifying static conditions and steady-state distributions of density and temperature, we obtain all the energies of the configuration and the predictions of the configuration we wish to study as output. In Table III, we observe the difference in energies of decay between the neutral state, when the electron is bound to the K shell, and the L shell (only for $2s_{1/2}$) for the predominant decays of the major LLFPs mentioned earlier. As anticipated, the bound-state beta decay energy is highest when the electron is bound to the K shell compared to the neutral case. Additionally, for certain radioisotopes, the energy for the L shell closely approximates that of the neutral case.

Table III: Comparison of Q-Values for Decay in Neutral Atoms vs. Bare Atoms with an Electron to K or L Shells

| Nuclide | $Q_{neutral}$ (keV) | $Q_b$ K shell (keV) | $Q_b$ L shell (keV) |
|---|---|---|---|
| Se-79 | 150.6 | 162.75 | 150.06 |
| Sr-90 | 546 | 561.53 | 545.72 |
| Zr-93 | 90.8 | 77.42 | 59.91 |
| Tc-99 | 297.5 | 317.88 | 297.65 |
| Pd-107 | 34 | 57.64 | 34.47 |
| Sn-126 | 378 | 278.51 | 251.10 |
| I-129 | 188.9 | 183.13 | 152.26 |
| Cs-135 | 268.7 | 303.81 | 270.51 |
| Cs-137 | 1175.63 | 549.08 | 515.78 |
| Sm-151 | 76.6 | 122.42 | 79.79 |

To validate the accuracy of our method, we applied it to calculate the half-life of Dy-163 and Re-187 and determined that our results align with those obtained experimentally, as demonstrated in Table IV.

Table IV: Impacts of BSBD on Bare LLFP Half-life

| Nuclide | Our Calculations $T_{1/2}^{BSBD}$ (Years) | GSI Experiment $T_{1/2}^{BSBD}$ (Years) |
|---|---|---|
| Dy-163 | 49.39 | 47 ± 3 |
| Re-187 | 32.12 | 32.9 ± 2 |

Our initial findings for the half-life of LLFPs are presented in Table V, detailing bare nuclides transitioning from the ground state to either a ground state or an excited state. The outcomes significantly differ from our expectations. We anticipated their half-lives to be even shorter than those indicated in Table II. In contrast, in some instances, their half-life is even longer than in the neutral case. One potential explanation might involve the existence of diverse couplings between the parent and daughter nuclear levels, under plasma conditions, which we did not consider. This suggests that different combinations could lead to different types of transitions, potentially resulting in lower comparative half-lives compared to those observed when the parent nucleus is in its ground state. Note that, in the present study, we used experimental quantities such as Q value, comparative half-life, and branching, which have uncertainties even up to the first decimal place.

Table V: Impacts of BSBD on bare LLFP half-life

| Nuclide | Type of transition | $T_{1/2}^{BSBD}$ K shell (Year) | $T_{1/2}^{BSBD}$ L shell (Year) |
|---|---|---|---|
| Se-79 | u | 1.24E+6 | 1.29E+07 |
| Sr-90 | u | 2.5E+2 | 2.09E+03 |
| Zr-93 | u | 3.4E+6 | 7.00E+07 |
| Tc-99 | nu | 2.99E+5 | 2.49E+06 |
| Pd-107 | u | 3.77E+5 | 2.12E+08 |
| Sn-126 | nu | 3.2E+5 | 2.78E+06 |
| I-129 | nu | 2.25E+6 | 2.27E+07 |
| Cs-135 | nu | 8.11E+5 | 7.04E+06 |
| Cs-137 | u | 1.07E+2 | 9.44E+02 |
| Sm-151 | nu | 1.21E+1 | 1.88E+02 |

## 3. Conclusions

The fundamental concept of BSBD was presented along with its potential effects on the half-life of major LLFPs. Additionally, the BSBD concept was employed in the context of fully ionized atoms utilizing the Takahashi-Yokoi model. Although our initial findings were not as anticipated, they prompted us to reconsider other factors that need to be incorporated into our future research endeavors. Ultimately, The BSBD process could potentially open a path towards a genuinely sustainable nuclear fuel cycle in the future.

## REFERENCES

[1] R. Daudel, M. Jean, and M. Lecoin, J. Phys. Radium 8, 238 (1947).
[2] M. Jung et al., Phys. Rev. Lett. 69, 2164 (1992).
[3] F. Bosch et al., Phys. Rev. Lett. 77, 5190 (1996).
[4] Yonghee Kim and SunjooYoon, "Ultra-accelerated Decay of Long-lived Fission Products via Bound-State Beta Decay", (2022).
[5] K. Takahashi, K. Yokoi, At. Data Nucl. Data Tables 36 (1987) 375.
[6] Shuo Liu, Chao Gao, and Chang Xu," Investigation of bound state $\beta-$ decay half-lives of bare atoms", (2021).
[7] Steffen Turkat, Xavier Mougeot, Balraj Singh, Kai Zuber, "Systematics of $log\ ft$ values for $\beta-$, and EC/$\beta+$ transitions", (2023).
[8] H. K. Chung, R. W. Lee, M. H. Chen, Y. Ralchenko, "The How To For FLYCHK", (2008).